

AD-A101 426

NAVAL RESEARCH LAB WASHINGTON DC
STABILITY CONSIDERATIONS FOR LIGHT-ION BEAM TRANSPORT IN Z-DISC--ETC(U)

F/G 20/7

NL

UNCLASSIFIED

NRL-MR-4548

1 of 1
400
10-220

END
DATE FILMED
[] -81
DTIC

O)

AD A101426

SECURITY CLASSIFICATION OF THIS PAGE (When Data Entered)

REPORT DOCUMENTATION PAGE		READ INSTRUCTIONS BEFORE COMPLETING FORM
1. REPORT NUMBER NRL Memorandum Report 4548	2. GOVT ACCESSION NO. <i>AD-A108-426</i>	3. RECIPIENT'S CATALOG NUMBER
4. TITLE (and Subtitle) STABILITY CONSIDERATIONS FOR LIGHT-ION BEAM TRANSPORT IN Z-DISCHARGE CHANNELS	5. TYPE OF REPORT & PERIOD COVERED Interim report on a continuing NRL problem	
6. AUTHOR(s) <i>P.F. Ottinger, D. Mosher, A. Goldstein*</i> <i>Sh</i>	7. PERFORMING ORG. REPORT NUMBER	
8. PERFORMING ORGANIZATION NAME AND ADDRESS Naval Research Laboratory Washington, D.C. 20375	9. PROGRAM ELEMENT, PROJECT, TASK AREA & WORK UNIT NUMBERS Sponsor Assignment No. DE-A108-79DP40092 NRL Prob 47-0879-0-1	
10. CONTROLLING OFFICE NAME AND ADDRESS Department of Energy Washington, D.C. 20545	11. REPORT DATE <i>July 8, 1981</i>	
12. MONITORING AGENCY NAME & ADDRESS (if different from Controlling Office) <i>14) NRL-MR-4548</i>	13. NUMBER OF PAGES 25	
14. DISTRIBUTION STATEMENT (of this Report) Approved for public release; distribution unlimited.	15. SECURITY CLASS. (of this report) UNCLASSIFIED	
16. DISTRIBUTION STATEMENT (of the abstract entered in Block 20, if different from Report)	15a. DECLASSIFICATION/DOWNGRADING SCHEDULE	
17. SUPPLEMENTARY NOTES *Present address: Jaycor, Inc., Alexandria, VA 22304	18. KEY WORDS (Continue on reverse side if necessary and identify by block number) intense ion beams transport instabilities z-discharge channels	
19. ABSTRACT (Continue on reverse side if necessary and identify by block number) Light-ion beams, appropriate for use as inertial-confinement fusion drivers, can be transported in z-discharge channels over distances of several meters. Here stability considerations for light-ion beam transport in such channels are reviewed. Many aspects of the important velocity-space instabilities are considered and the resulting conditions for good transport are discussed. The results will be presented in a general form so that they may be applied to beams of various species (e.g. H ⁺ , D ⁺ , C ⁺⁴ , etc.) propagating in channel plasmas of different composition (e.g. hydrogen, argon, air, etc.).		

DD FORM 1 JAN 73 1473

EDITION OF 1 NOV 65 IS OBSOLETE

S/N 0102-014-6601

SECURITY CLASSIFICATION OF THIS PAGE (When Data Entered)

CONTENTS

1. INTRODUCTION	1
2. BEAM-PLASMA SYSTEM IN THE TRANSPORT CHANNEL	2
3. LINEAR STABILITY ANALYSIS	3
3.1. <u>ES Modes</u>	4
3.1a. <u>e-b Two Stream Mode</u>	4
3.1b. <u>e-i Two Stream Mode</u>	5
3.1c. <u>Ion-Acoustic Mode</u>	5
3.1d. <u>ES Stability Conditions</u>	6
3.2. <u>EM Modes</u>	6
3.2a. <u>Beam-Whistler Mode</u>	6
3.2b. <u>Beam-Weibel Mode</u>	7
3.2c. <u>Plasma-Electron Mode</u>	7
3.2d. <u>EM Stability Conditions</u>	8
4. CONCLUSIONS	9
5. REFERENCES	10

Accession For	
MITS GRS&I	<input checked="" type="checkbox"/>
LTRIC TAB	<input type="checkbox"/>
Unpublished	<input type="checkbox"/>
Justification	<input type="checkbox"/>
Prepared by	
Distribution by	
Availability Codes	
Dist	Avail and/or Special
A	

STABILITY CONSIDERATIONS FOR LIGHT-ION BEAM TRANSPORT IN Z-DISCHARGE CHANNELS

1. INTRODUCTION

The development of terawatt-level ion beams has generated a great deal of interest in using light-ion beams to drive thermonuclear pellets.¹⁻⁹ Target design studies for light-ion beams indicate that ~ 2 MJ of ions must be delivered in ~ 10 nsec to an ~ 1 cm diameter pellet in order to achieve high-gain thermonuclear ignition.¹⁰ Since present technology can provide up to 5 TW single-generator modules from which up to 200 kJ of ions can be extracted in ~ 50 nsec, a multimodule system is required. In addition, a transport scheme and a method for beam pulse compression are needed.

One possible transport scheme involves the use of a z-discharge channel for transporting a prefocused ion beam (Fig. 1).¹¹ Focusing is achieved by a combination of geometric and magnetic-field focusing prior to injection into the channel.^{12,13} Beam pulse compression results from ramping the diode voltage such that the tail of the beam catches up to the front of the beam.^{13,14} The ideal diode voltage waveform is $\phi(t) = \phi_0(1-t/t_a)^{-2}$ for $0 \leq t \leq \tau_b < t_a$ where τ_b is the beam pulse duration and t_a is the beam arrival time at the target.

Assuming that the z-discharge channel is produced in a MHD stable configuration, the question of the effects that the passage of the beam will have on the equilibrium and stability of the beam-plasma system is an important one. The MHD response of the plasma has been treated elsewhere¹⁵ and will only be briefly reviewed here. Analysis of stable beam propagation in straight and tapered channels, as well as in bumpy channels (subject to sausage instability) has also been done previously.¹⁶ This work shows that, in the absence of microinstabilities driven by the beam, good beam transport and bunching is possible under the conditions set by MHD considerations (which will be outlined in Sec. 2). However, in the presence of microinstabilities, beam transport and bunching can be seriously affected.

Analysis of electrostatic (ES)¹⁷ and electromagnetic (EM)¹⁸ velocity-space instabilities, which can grow on a time scale much faster than the beam pulse duration, will be reviewed in this report. The problem will be considered with the goal of identifying the conditions for good transport and bunching. The results will be presented in a general form so that they may be applied to beams of various low atomic number species propagating in channel plasmas of different compositions.

2. BEAM-PLASMA SYSTEM IN THE TRANSPORT CHANNEL

The beam-plasma system consists of a focused ion beam propagating down the axis of an externally-driven z-discharge plasma channel.^{13,19} The ion beam is focused at the entrance to the plasma channel (see Figs. 1 and 2) with velocity components transverse to z given by $V_\perp/V_z = \tan \alpha \ll 1$. The current being driven in the preformed z-discharge channel provides the radial confinement of the beam. Because of the small perpendicular beam energy, the channel current can be much less than the beam current. A high plasma density in the channel insures good beam charge neutralization.²⁰ Good beam current neutralization in the interior of the beam also occurs, so that the total magnetic field is comparable to that associated with the preformed channel established before beam injection. Because $J_p = J_{ch} - J_b = -J_b$, the electron drift velocity is approximated by $V_e \approx n_b Z_b V_b / Z_p n_p$, where n_b and n_p are the beam and plasma ion densities, Z_b and Z_p are the beam and plasma ion charge states, and J_p , J_b and J_{ch} are the plasma, beam and preformed channel current densities, respectively. Note that the electron density is $Z_p n_p$.

Hydrodynamic modeling of the background plasma¹⁵ shows that a uniform net-current model is appropriate for the early times associated with passage of the beam front. This is because the low-temperature channel is established microseconds before beam injection so that complete magnetic diffusion occurs. Later in the ion pulse, $J_p \times B$ expansion of the beam-heated high-temperature plasma reduces the magnetic field strength in the interior of the channel. The built-up field in the expanding cylindrical shock wave is also enhanced by significant current non-neutralization in the cool plasma surrounding the beam-heated channel. The maximum field strength just outside the ion-beam radius can exceed that established by the preformed z-discharge current by a large factor. Thus, at late times during beam passage, the magnetic field distribution can be approximated by a surface-current model. Although the induced $V_r \times B_\theta$ electric field is important when considering beam energy losses during transport, at no time does the electric field become large enough to significantly affect the stability analysis.

The linearized stability analysis presented here strictly applies only when the mode under consideration grows on a time scale faster than any changes in the beam-plasma system (i.e., $\gamma > \tau_b^{-1}$). For growth on a time scale slower than the beam pulse duration, the perturbation analysis breaks down since small perturbations will be washed out by the zero-order changes in the system before growth can occur. Thus for those modes which are shown to e-fold less than once during the passage of the beam, the results should be interpreted as showing that significant growth does not occur.

The distribution of particles in axial velocity is illustrated in Fig. 3. The plasma ions form a stationary background while the drift of the plasma electrons provides for beam current neutralization. Because of the high plasma density, this drift velocity, V_e , does not exceed the electron thermal velocity even before the beam heats the plasma. As the beam passes through a given point, the plasma is heated and the conductivity increases. The electron-ion collision frequency, ν_{ei} , decreases but the electrons generally remain collisional ($\nu_{ei} > \omega_{ce}$) at all times during the pulse for purposes of the stability analysis. Since the electron-ion equilibration time is on the order of the beam pulse duration the electron temperature will not exceed the ion temperature by more than a factor of ten.

The ion beam density is typically much less than the plasma density and, beams of interest are nonrelativistic. The spread in axial velocities, designated by V_t in Fig. 3, is on the order of $V_b \alpha_m^2 / 2$ before beam bunching occurs. Here V_b is the beam velocity and α_m is the maximum ion injection angle into the channel. For $\alpha_m = 0.1-0.2$ rad, V_t/V_b is relatively small. As the beam bunches, V_t/V_b can increase by an order of magnitude as the faster ions generated later in the pulse catch up to slower ions at the front of the beam. The beam pulse duration, τ_b , decreases and the beam density, n_b , increases as the beam bunches. The dependence of the beam parameters on axial position due to bunching will be expressed explicitly as $V_t(z)$, $\tau_b(z)$, etc.

Since the ES stability analysis depends strongly on the shape of the beam distribution function, it is important to use a theoretical model which contains the appropriate physics. For a distribution in v_z which has a large slope on the low velocity side such as illustrated in Fig. 4a, a resistive instability persists in spite of the thermal spread in v_z and the high frequency of collisions between the plasma electrons and ions.^{21,22} However, if the slope of the distribution function is not as sharp, such as for the Gaussian distribution shown in Fig. 4b, electron-ion collision are damping if the thermal spread in v_z is sufficiently large. The slope of the distribution function on the high velocity side does not affect the stability analysis.

Before the beam bunches, the distribution in v_z is determined by the injection condition. Since the ions are injected into the channel nearly uniformly over a range of angles predominately in the r-z plane and since the time-averaged axial velocity for an ion injected at a given α varies like $V_t(1-\alpha^2/2)$, the distribution in v_z rises slowly as indicated in Fig. 4c. Additional smoothing out of the distribution in v_z will result from beam energy spreading due to radial variations in the diode voltage. The stability properties of this distribution closely resemble those of the Gaussian distribution. The beam ion distribution after bunching is also similar in shape to Fig. 4c. Since the ion diodes which are used in the experiments have a constant impedance behavior during the duration of the ion pulse, more ions (higher currents) are generated at higher energies as the diode voltage ramps upward. Thus in the bunched state there are more ions at higher velocities than at lower velocities and the spread in axial velocities is on the order of $(2Z_{de}/m_1)^{1/2}(\phi_f^{1/2}-\phi_o^{1/2})$. Here Z_d is the charge state of the beam ions in the diode and ϕ_o and ϕ_f are the initial and final diode voltages. This spread can be considerably larger than the initial spread before bunching ($V_t \sim V_b \alpha_m^2 / 2$).

Thus a Gaussian distribution can be used to properly model the ion beam distribution function both before and after bunching when considering ES modes. When the analysis is not sensitive to the detailed shape of the distribution function (e.g. for analyzing the stability of EM modes), simpler models may be used.

3. LINEAR STABILITY ANALYSIS

The results of linear stability analyses reported previously^{17,18,22} are presented here in a more general form so that they may be applied to beams of various species. The composition of the channel plasma is also unspecified. Growth rates will vary as the beam heats the channel plasma and as the channel expands. The changes in the hydrodynamic structures of

the channel occur gradually over the pulse duration of the beam. Growth rate expressions appropriate near both the front and the tail of the beam are presented in order to determine how hydrodynamic changes alter the results. Most notably these changes include (1) a reduction in the e-i collision frequency at the tail of the beam where the plasma is heated, and (2) a reduction in the magnetic field in the interior of the channel at late times in the pulse as the now highly conducting heated plasma expands due to $\mathbf{J} \times \mathbf{B}$ forces. Near the front of the beam, the beam ions follow betatron-like orbits while at the tail of the beam, the beam ions move in more straight line-like orbits with reflections off of the magnetic field piled up at the edge of the channel.

3.1. ES Modes

The ES modes are the fastest growing modes when driven unstable. Unstable growth will generally reach nonlinear saturation on a time scale much faster than the beam pulse duration. These modes involve either charge bunching (e-b and e-i modes) or density bunching (ion-acoustic mode) and generally exhibit their largest growth for $k = k_{\parallel}$, which is a result of the small thermal spread in the axial direction before axial beam compression occurs.

3.1a. e-b Two Stream Mode

The e-b two stream instability is driven by the relative streaming between the beam ions and plasma electrons. In general the beam can be considered warm because $V_t(z)/V_b \gtrsim 2[m_e Z_b^2 n_b(z)/m_b Z_p n_p]^{1/3}$ even before beam bunching occurs. Here m_b is the beam ion mass. Near the front of the beam the betatron motion of the ions can reduce the growth rate of the mode which is given by

$$\gamma_1 = -\frac{\nu_{ei}}{2} + 0.76 \frac{\omega_{pb}^2(z)}{\omega_{pe}^2} \left(\frac{V_b}{V_t(z)} \right)^2 R \quad (1)$$

where $\omega_{pb}^2 = 4\pi e^2 Z_b^2 n_b(z)/m_b$ and $\omega_{pe}^2 = 4\pi e^2 Z_p^2 n_p/m_e$ are the beam and electron plasma frequencies respectively. The electron-ion collision frequency is given by $\nu_{ei} = 1.45 \times 10^{-6} Z_p^2 n_p \lambda_{ei} / T_e^{3/2}$, where T_e is in eV and λ_{ei} is the Coulomb logarithm. The reduction factor, R , equals the fraction of beam ions which can effectively participate in the wave growth. If $\gamma_1 > 2\omega_B$, which is the usual case, all ions can participate and $R = 1$. Here $\omega_B = (V_b \omega_{cb} / r_c)^{1/2}$ is the ion betatron frequency and ω_{cb} is the beam cyclotron frequency. If $\gamma_1 \leq 2\omega_B$, only those ions with $\Delta z < 1/k$ can participate, where Δz is the amplitude of the betatron oscillations about $z = V_t t$ (see Fig. 5). The amplitude, Δz , depends on the ion injection conditions, $r(z=0)$ and $\alpha(z=0)$. If this amplitude is large, the ion moves across many wave fronts before the instability e-folds even once, and thus cannot effectively participate in wave growth. The value of R must be calculated from the actual distribution function. For a Gaussian distribution $R \sim 8\omega_B V_b / k V_t^2$ for $k > 8\omega_B V_b / V_t^2$ and $R = 1$ for $k < 8\omega_B V_b / V_t^2$. At the tail of the beam, betatron effects are less important, so that $R = 1$ in Eq. (1).

Beam heating of the plasma can considerably reduce the damping term in Eq. (1) as e-i collisions become less frequent. Beam bunching, on the other hand, reduces the driving term in Eq. (1) as V_t increases dramatically. Thus the potentially most dangerous position for wave growth lies at the tail of the beam ($R=1$) at the beginning of the transport channel before significant beam bunching occurs.

3.1b. e-i Two Stream Mode

The e-i two stream mode is driven by the relative streaming between the background electrons and ions. The electrons drift with an average velocity $V_e \sim n_b Z_b V_b / Z_p n_p$ relative to the stationary ions and in general $V_e < u_e$. Here u_e is the thermal velocity of the electrons. The expression for the growth (damping) rate is

$$\gamma = -v_{ei} - (\pi/8)^{1/2} \frac{k c_s}{(1+k^2 \lambda_{De}^2)^{3/2}} \left\{ Z_p (T_e/T_i)^{3/2} \exp \left[-\frac{T_e}{2T_i (1+k^2 \lambda_{De}^2)} \right] + \frac{m_e}{m_i} \left(1 - \frac{V_e}{c_s} \left[1+k^2 \lambda_{De}^2 \right]^{1/2} \right) \right\} \quad (2)$$

where $c_s = (T_e/m_i)^{1/2}$ is the ion sound speed, $\lambda_{De} = (T_e/4\pi e^2 Z_p n_p)^{1/2}$ is the electron Debye length and where a simple Krook model was used for the collision term. In deriving Eq. (2), it was assumed that $v_{ei} < k c_s / (1+k^2 \lambda_{De}^2)^{1/2}$. When $T_e \sim T_i$ this reduces to

$$\gamma_2 \approx -v_{ei} + (\pi/8)^{1/2} \frac{k c_s}{(1+k^2 \lambda_{De}^2)^{3/2}} \left\{ \frac{V_e}{u_e} - \frac{Z_p \exp \left[-\frac{1}{2(1+k^2 \lambda_{De}^2)} \right]}{(1+k^2 \lambda_{De}^2)^{1/2}} \right\} . \quad (3)$$

Since V_e is usually less than u_e , the mode is typically stable.

3.1c. Ion-Acoustic Mode

If $T_e \gg T_i$, then the drifting electrons can drive an ion-acoustic instability. In this case Eq. (2) reduces to

$$\gamma_3 \approx -v_{ei} + \left(\frac{\pi m_e}{8 m_i} \right)^{1/2} \frac{k}{(1+k^2 \lambda_{De}^2)^{3/2}} \left[V_e - \frac{c_s}{(1+k^2 \lambda_{De}^2)^{1/2}} \right] \quad (4)$$

This predicts instability ($\gamma > 0$), if $V_e/c_s > (1+k^2 \lambda_{De}^2)^{-1/2}$ and if v_{ei} is sufficiently small. However, the severity of the condition on T_e/T_i is often overlooked. For V_e/c_s as large as 5, T_e/T_i must be greater than 12 for instability even for $k\lambda_{De} \ll 1$. Figure 6 shows the critical values of T_e/T_i for instability versus k for various values of V_e/c_s (assuming $v_{ei} = 0$). Since T_e/T_i is not expected to reach such high levels, in general ion-acoustic turbulence is not expected.

3.1d. ES Stability Conditions

Since the e-b mode is the only ES instability which could be generated, it is important to state under which conditions it may be avoided. For stability ($\gamma_1 \leq 0$) Eq. (1) states that

$$\frac{z_p^{5/2} n_p^{3/2} \lambda_{ei}}{T_e^{3/2}} \geq 3.2 \times 10^7 \frac{z_b^2 n_b(z) v_b^2}{\mu_b v_t^2(z)} \quad (5)$$

is required. Here $\mu_b = m_b/m_i$, T_e is measured in ev and all other variables are in Gaussian units. This condition used in conjunction with the condition

$$n_p \approx 1.4 \times 10^{12} I_{ch} r_{ch}^{-2} (I_b(z) \tau_b(z)/S)^{\frac{1}{2}}, \quad (6)$$

derived from MHD considerations¹⁵, set constraints on n_p and T_e for good transport. Here I_{ch} and I_b are measured in amps and S is the beam stopping power of the plasma measured in erg·cm²/g. Eq. (6) gives the ion density in the channel required for minimum beam energy loss in the channel during transport. Given this required ion density, Eq. (5) sets an upper limit on T_e , beyond which electrostatic turbulence will set in. For good transport both of these conditions must be satisfied. Generally the stability criterion in Eq. (5), is most severely tested at the tail of the beam where T_e is largest and at the beginning of the transport channel before significant bunching occurs where $v_t(z)$ is smallest ($v_t(z)/v_b \sim \alpha_m^2/2$).

3.2 EM Modes

The EM modes are slower growing modes than the ES modes, so that even if the mode is unstable, growth may not have sufficient time to reach non-linear saturation during the pulse duration of the beam. The modes are nearly purely growing (i.e. do not convect with the beam) and involve current bunching or filamentation of the beam and/or plasma channel. The wave vector, \mathbf{k} , is oriented perpendicular to the direction of beam propagation with $\mathbf{k} = k_r \hat{\mathbf{e}}_r$ for the Weibel mode (radial current bunching) and $\mathbf{k} = k_\theta \hat{\mathbf{e}}_\theta$ for the whistler mode (azimuthal current bunching). In addition, the cylindrical geometry dictates that $k_r \geq 2\pi/r_b$ and $k_\theta \geq l/r_b$ where l is an integer.

3.2a. Beam-Whistler Mode

The beam-whistler instability is driven unstable by the relative streaming motion between the beam ions and the channel plasma. Since the wave vector is in the azimuthal direction and the beam ions execute their betatron orbits in the $r-z$ plane, the betatron motion of the beam has little effect on the mode. However, a small spread in angular momentum, which is observed experimentally, can reduce the growth rate significantly. With no spread in angular momentum ($v_\theta^2/c^2 < 2v_{ei}w_{pb}v_b/cw_{pe}^2$) the growth rate is

$$\gamma = \omega_{pb}(z)v_b/c, \quad (7)$$

and with $v_\theta^2/c^2 > 2v_{ei}\omega_{pb}(z)v_b/c\omega_{pe}^2$ the peak growth rate is

$$\gamma_4 = 2v_{ei}\omega_{pb}^2(z)v_b^2/v_\theta^2\omega_{pe}^2 \quad (8)$$

at $k \sim \gamma_4/v_b$. Here v_θ is a measure of the thermal spread in the azimuthal velocity of the beam ions. If $k r_b < 1$, peak growth rate is reduced to $[1-(k_0 r_b)^{-2}] \gamma_4$ because of geometry constraints and if $k_{orb} < 1$, no growth is possible. The critical wavenumber $k_0 = \sqrt{2\omega_{pb}(z)v_b/cv_\theta}$ [see Eq. (35), Ref. 18].

If there is wave growth at a given point in z , the number of e-folds that occurs is just

$$N = \int_0^{r_b(z)} \gamma(t) dt, \quad (9)$$

where the time dependence of the plasma parameters must be considered. Most importantly v_{ei} decreases at $T_e^{-3/2}(t)$ as the plasma is heated by the passing beam. Note that beam thermal effects do not completely quench the instability because of the finite plasma resistivity. Given information from MHD considerations on the time variation of the plasma parameters due to beam passage, one can then determine from Eq. (9) whether significant azimuthal beam current bunching occurs.

3.2b. Beam-Weibel Mode

For the beam-Weibel instability the wave vector is in the radial direction. In this case the spread in perpendicular velocities associated with the betatron motion of the beam ions reduces the growth rate of the instability. A measure of the radial velocity spread is given by $v_{o\alpha_m}$, so that the peak growth rate is given by

$$\gamma_5 = 2^{4/5} v_{ei} \omega_{pb}^2(z) / \omega_{pe}^2 \alpha_m^{8/5} \quad (10)$$

at $k \sim \gamma_5/v_{b\alpha_m}^{7/5}$. Again the number of e-folds that occur at a given point in z can be determined by Eq. (9) and MHD considerations. Since the thermal spread in the radial velocity is typically comparable or larger than the thermal spread in the azimuthal velocity, the beam-Weibel instability is generally less dangerous than the beam-whistler mode. A superposition of both unstable modes, however, will lead to beam filamentation.

3.2c. Plasma-Electron Mode

If beam thermal effects or geometry constraints prevent the beam from driving strong EM wave growth, instability can still result from the electron return current established with the plasma. Because of the high collisionality ($v_{ei} > \omega_{ce}$) of the plasma electrons, radial ($\mathbf{k} = \hat{\mathbf{k}}_r$) and azimuthal ($\mathbf{k} = \hat{\mathbf{k}}_\theta$) EM modes driven by the plasma electrons are essentially indistinguishable (aside from small geometric effects). The analysis must include electron thermal effects, as well as collisional effects since the

electron streaming velocity is subthermal even early in the pulse before beam heating occurs.

At early times in the pulse when $\omega_{pe}u_e/cv_{ei} > 1$, the peak growth rate is

$$\gamma = (\omega_{pe}V_e/c)(2-z_p^{-1})^{1/2} . \quad (11)$$

Later in the pulse after the beam heats the plasma if $\omega_{pe}u_e/cv_{ei} > 1$, then thermal effects slows the growth of the mode. The maximum growth rate is then given by

$$\gamma = 2^{-3/2}\omega_{pe}V_e^2/cu_e . \quad (12)$$

At all times in the pulse geometry constraints prevent wave growth if $k_{orb} < 1$ where in this case $k_o = \omega_{pe}V_e/\sqrt{2}u_{ec}$. Since again this mode does not convect, the number of e-folds at a given point in z can be obtained from Eqs. (11), (12) and (9) and MHD considerations.

3.2d. EM Stability Conditions

If the growth rates of the EM instabilities are slow enough such that less than one e-fold ($N < 1$) occurs during beam passage, wave growth will be washed out by the MHD changes in the beam-plasma system. Only wave growth with $N > 1$ will affect beam transport. In order to prevent the beam from filamenting, the beam should then have

$$\alpha_m^2 \gtrsim V_\theta^2/V_b^2 > 1.6 \times 10^{-9} \frac{n_b(z)}{\mu_b} \int_0^{\tau_b(z)} \left(\frac{z_p \lambda_{ei}}{T_e^{3/2}} \right) dt , \quad (13)$$

where again T_e is in eV's and n_b is measured in cm^{-3} . This condition is derived from Eq. (8) for azimuthal current bunching which is typically more severe than the condition for radial current bunching since α_m is usually greater than V_θ/V_b . Here it is also assumed that $\sqrt{2}\omega_{pb}(z)r_bV_b/cV_\theta > 1$, which is the usual case. In order to evaluate Eq. (13), a knowledge of the MHD response to beam passage is required, in particular, one must know the time history of the electron temperature.

If the beam is warm enough to prevent beam filamentation (i.e., Eq. (13) is satisfied), it is still possible for the channel to filament. Channel filamentation is avoided if

$$\frac{J_b(z)}{n_p} \left(\frac{9.4 \times 10^1}{\mu_p} \int_0^{t_1(z)} (2-z_p^{-1}) dt + 6.9 \times 10^4 J_b(z) \int_{t_1(z)}^{\tau_b(z)} \frac{dt}{n_p z^{3/2} T_e^{1/2}} \right) \leq 1 . \quad (14)$$

Here $\mu_p = m_p/m_H$, $J_b(z) = \Sigma_b n_b(z) V_b$, J_L is measured in sA/cm^2 and t_1 is defined as the time it takes for the beam to heat the plasma

to $T_e^1 = 1.4 \times 10^{-4} (Z_p^3 t_1 n_p \lambda_e^2)^{1/4}$ in eV. If $T_e(0) > T_e^1$, then $t_1 = 0$ and the first term in Eq. (14) does not contribute. If $t_1 \geq \tau_b$, then the second term in Eq. (14) does not contribute and the limits on the integration of the first term go from 0 to $\tau_b(z)$. In Eq. (14) it was assumed the $\omega_{pe} V_e / 2u_e c > 1$, which is the usual case. Eq. (14) sets an upper limit on transportable beam current density above which channel filamentation will develop.

4. CONCLUSIONS

The stability conditions in Eqs. (5), (13) and (14), identify important constraints on beam propagation. Eq. (5) together with Eq. (6) states that the plasma cannot be heated above a certain critical temperature without generating electrostatic microturbulence. Such turbulence will degrade beam quality and confinement. In general the most severe constraint on T_e exists at the tail of the beam before bunching occurs where the critical temperature is defined by

$$T_e^c (\text{eV}) \equiv 10^{-6} \left(\frac{\mu_b^2 n_p^3 Z_p^5 \lambda_e^2 \alpha_m^8}{Z_b^4 n_b^2 (z=0)} \right)^{1/3}, \quad (15)$$

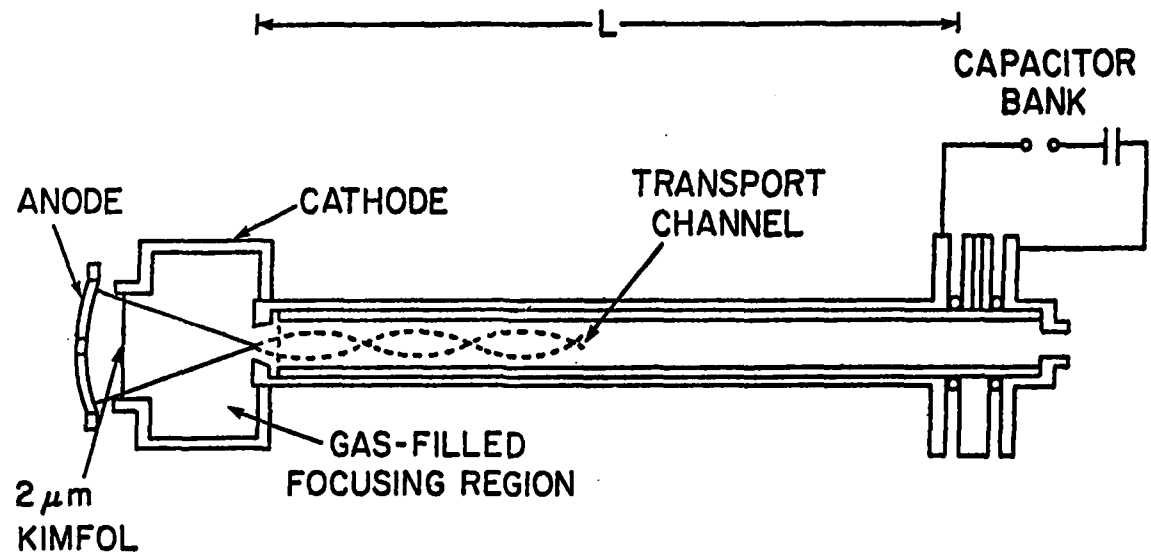
where n_p is given in Eq. (6). By increasing n_p the critical temperature can be raised at the expense of increasing the beam energy loss during transport. Operating at twice the density specified in Eq. (6) increases T_e^c by a factor of two but only increases the beam energy loss by 25%. The actual temperature that the electrons will reach for a given beam and background gas is not always easily estimated and must be calculated on a case to case basis and compared with the critical temperature defined in Eq. (15). Here α_m is a measure of the spread in axial velocities in the beam, which for a monoenergetic beam is given by $\Delta V_z / V_b \sim \alpha_m^2 / 2$. If the beam has a spread in energy such that $\alpha_m^2 < \Delta E / E$, then α_m^8 in Eq. (15) should be replaced by $(\Delta E / E)^4$.

Growth of electromagnetic waves can be held to a tolerable level by allowing for a reasonable spread in beam perpendicular energy and limiting the beam current density. If the beam is too cold, beam filamentation can occur during beam transport. The condition for good beam transport is given in Eq. (13). If the beam does not filament but the beam current density is too high, the return current in the channel can cause channel filamentation. In order to prevent this from occurring Eq. (14) should be satisfied. The conditions given in Eqs. (13) and (14) may actually be too severe since channel hydrodynamic effects have not been included self consistently in the analysis. Channel expansion due to $J \times B$ force may tend to prevent growth of these transverse modes. These effects are presently under investigation.

5. REFERENCES

1. S. A. Goldstein and R. Lee, Phys. Rev. Lett. 35, 1079 (1975).
2. J. W. Poukey, J. R. Freeman, M. J. Clauser, and G. Yonas, Phys. Rev. Lett. 35, 1806 (1975).
3. J. W. Poukey, J. Vac. Sci. Technol. 12, 1214 (1975)
4. A. E. Blaugrund, G. Cooperstein, J. R. Boller and S. A. Goldstein Bull. Am. Phys. Soc. 20, 1252 (1975).
5. P. A. Miller, C. W. Mendel, D. W. Swain, and S. A. Goldstein, in Proceedings of the International Topical Conference on Electron Beam Research and Technology, Albuquerque, New Mexico (1975), p. 619.
6. G. Cooperstein, S. J. Stephanakis, J. R. Boller, R. Lee, and S. A. Goldstein, in Proceedings of the 1976 IEEE International Conference on Plasma Science, Austin, Texas (IEEE, New York, 1976), p. 126.
7. D. J. Johnson, G. W. Kuswa, A. V. Farnsworth, Jr., J. P. Quintenz, R. J. Leeper, E. J. T. Burns, and S. Humphries, Jr., Phys. Rev. Lett. 42, 610 (1979); D. J. Johnson, Bull. Am. Phys. Soc. 24, 925 (1979).
8. G. Cooperstein, S. A. Goldstein, D. Mosher, W. F. Oliphant, F. L. Sandel, S. J. Stephanakis and F. C. Young in Proceedings Third International Topical Conference on High Power Electron and Ion Beam Research and Technology, Novosibirsk, USSR (1979).
9. G. Cooperstein, S. A. Goldstein, D. Mosher, R. J. Barker, J. R. Boller, D. G. Colombant, A. Drobot, R. A. Meger, W. F. Oliphant, P. F. Ottlinger, F. L. Sandel, S. J. Stephanakis and F. C. Young, in Laser Interaction and Related Plasma Phenomena, edited by H. Schwarz, H. Hora, M. Lubin and B. Yaakobi, (Plenum Press, New York, 1980).
10. R. O. Bangerter and D. J. Meeker, in Proceedings of the Second International Topical Conference on High Power Electron and Ion Beam Research and Technology, Ithaca, New York (1977), p. 183; J. H. Nuckolls, in Proceedings of the Topical Meeting on ICF (Opt. Soc. of Am. Wash., DC, 1978) paper TuA5.
11. S. A. Goldstein, D. P. Bacon, D. Mosher and G. Cooperstein Proceedings of the Second International Topical Conference on High Power Electron and Ion Beam Research and Technology, Ithaca, New York (1977), p. 71.
12. D. Mosher, G. Cooperstein, S. A. Goldstein, in Digest of the Topical Meeting on ICF (Opt. Soc. of Am., Wash., DC, 1980), paper ThC5.
13. D. Mosher, Bull. Am. Phys. Soc. 24, 926 (1979).
14. D. Mosher and S. A. Goldstein, Bull. Am. Phys. Soc. 23, 800 (1978).

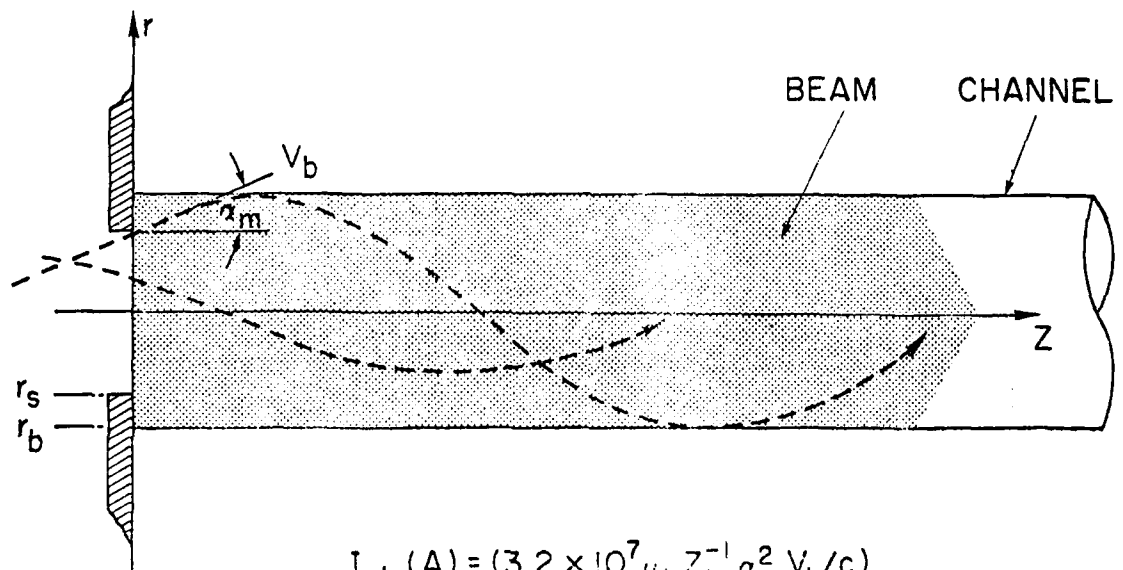
15. D. G. Colombant, D. Mosher and S. A. Goldstein, Phys. Rev. Lett. 45, 1253 (1980).
16. P. F. Ottinger, D. Mosher and S. A. Goldstein, Phys. Fluids 23, 909 (1980).
17. P. F. Ottinger, D. Mosher and S. A. Goldstein, Phys. Fluids 22, 332 (1979).
18. P. F. Ottinger, D. Mosher and S. A. Goldstein, Phys. Fluids 24, 164 (1981).
19. F. Sandel. G. Cooperstein, S. A. Goldstein, D. Mosher and S. J. Stephanakis, Bull. Am. Phys. Soc. 24, 1031 (1979).
20. D. A. Hammer and N. Rostoker, Phys. Fluids 13, 1831 (1970).
21. B. S. Newberger and L. E. Thode, Bull. Am. Phys. Soc. 24, 1097 (1979).
22. P. F. Ottinger, Conference Record-Abstracts of the 1980 IEEE International Conference on Plasma Science, Madison, Wisconsin (IEEE, New York, 1980), p. 57.
23. V. U. Abramovich and V. I. Sevchenko. JETP 35, 730 (1972).
24. P. F. Ottinger, S. A. Goldstein and D. Mosher, NRL Memorandum Report 4180 (1980).



IDEAL DIODE VOLTAGE WAVEFORM:

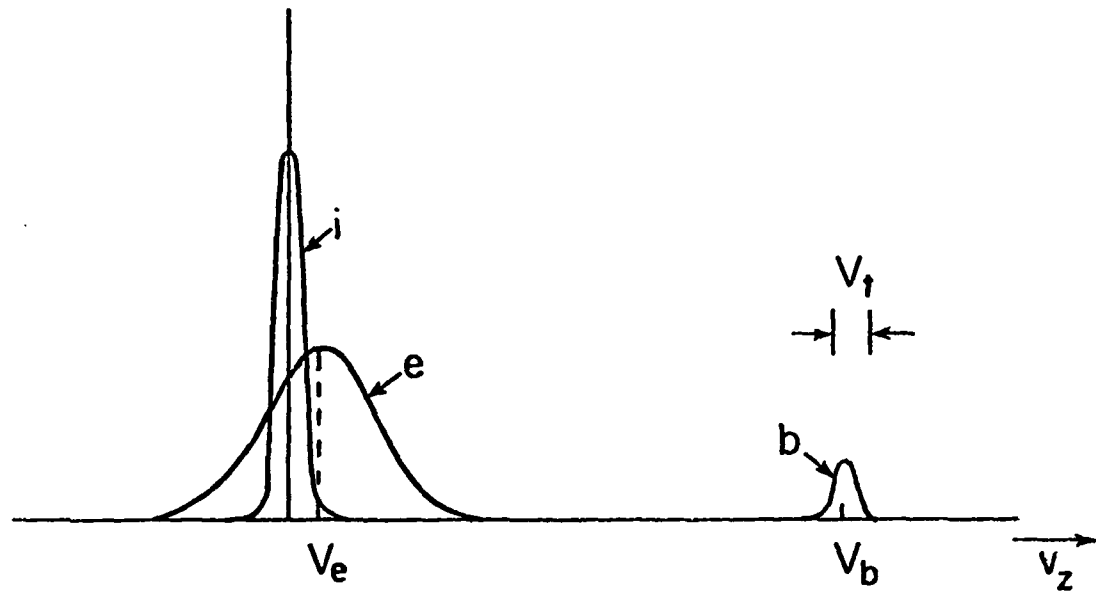
$$\phi(t) = \frac{\phi_0}{(1 - t/t_a)^2} ; \quad 0 \leq t \leq \tau_b < t_a$$

Fig. 1—Schematic of ion diode, focusing region and transport channel for light ion beam ICF module. The ideal diode voltage waveform for axial bunching is also shown where ϕ_0 is the initial diode voltage, t_a is the beam arrival time at the target and τ_b is the beam pulse duration at injection.



$$I_{ch} (A) = (3.2 \times 10^7 \mu_b Z_b^{-1} \alpha_m^2 V_b / c)$$

Fig. 2—Schematic of beam propagation in a z -discharge channel. Here $\frac{1}{2} m_i V_b = Z_d e \phi$ (where Z_d is beam ion charge state in the diode and ϕ is the diode voltage), α_m is the maximum injection angle, r_s is the beam spot size (or aperture size) and r_b is the beam radius in the channel. Also shown is the channel current required to confine the beam where Z_b is the charge state of the beam ions in the channel and $\mu_b = m_b/m_H$.



PLASMA:

$$T_e \gtrsim T_i$$

$$\nu_{ei}(T_e) > \omega_{ce}$$

$$V_e \approx Z_b n_b V_b / Z_p n_p < (T_e/m_e)^{1/2}$$

BEAM:

$$V_b/c \ll 1$$

$$n_b \ll n_p$$

$$\frac{V_t}{V_b} \approx a_m^2$$

Fig. 3—Schematic of particle distribution in v_z . Here i, e and b are the plasma ions, plasma electrons and beam ions, respectively, and V_t is the measure of the spread in the beam distribution. Other typical beam-plasma conditions are also listed.

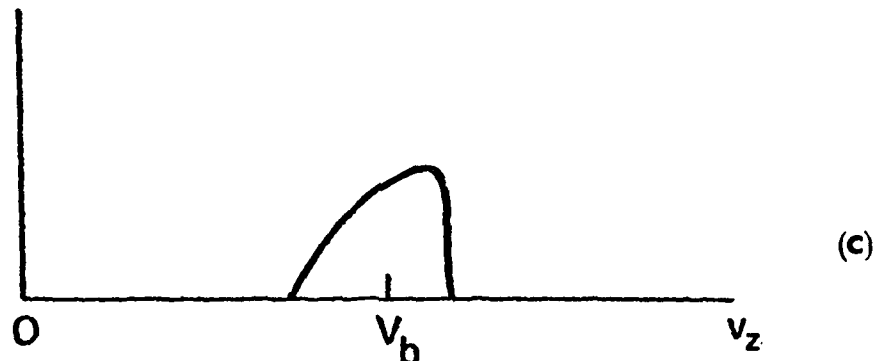
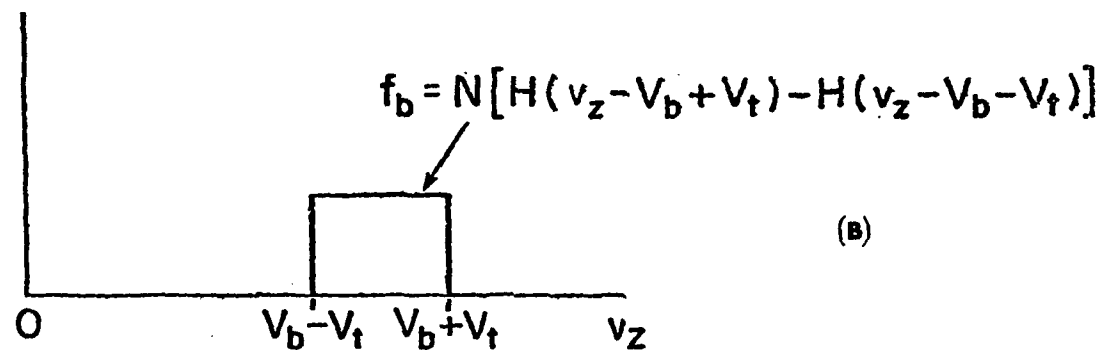
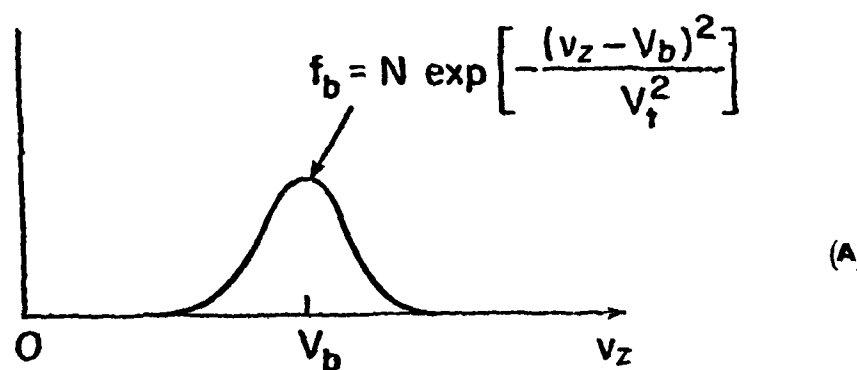


Fig. 4- Distribution of beam ions in v_z for (a) a uniform distribution, (b) a Gaussian distribution actual distribution and (c)

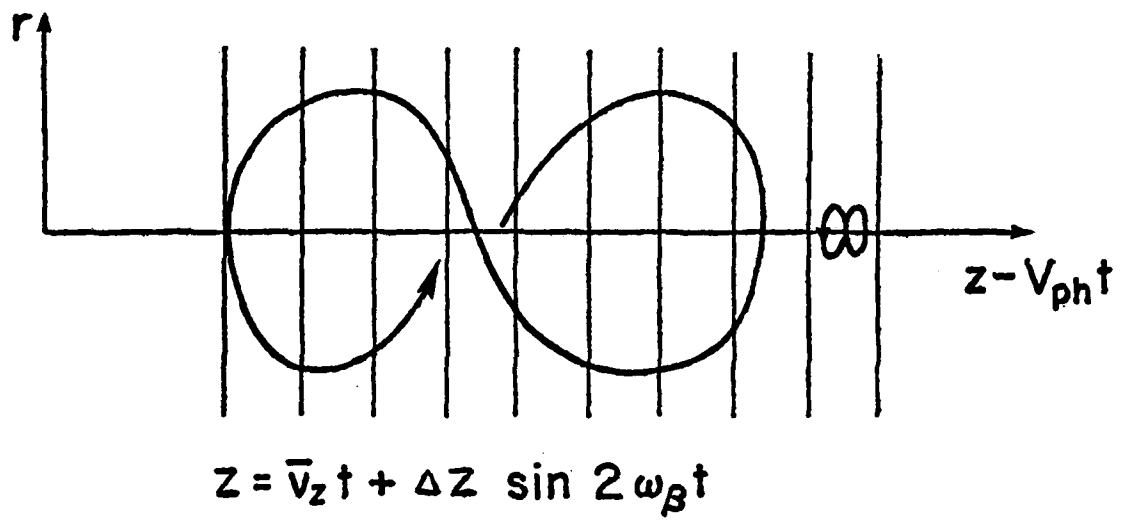


Fig. 5—Beam ion orbits in a frame of reference moving with the phase velocity of an ES wave

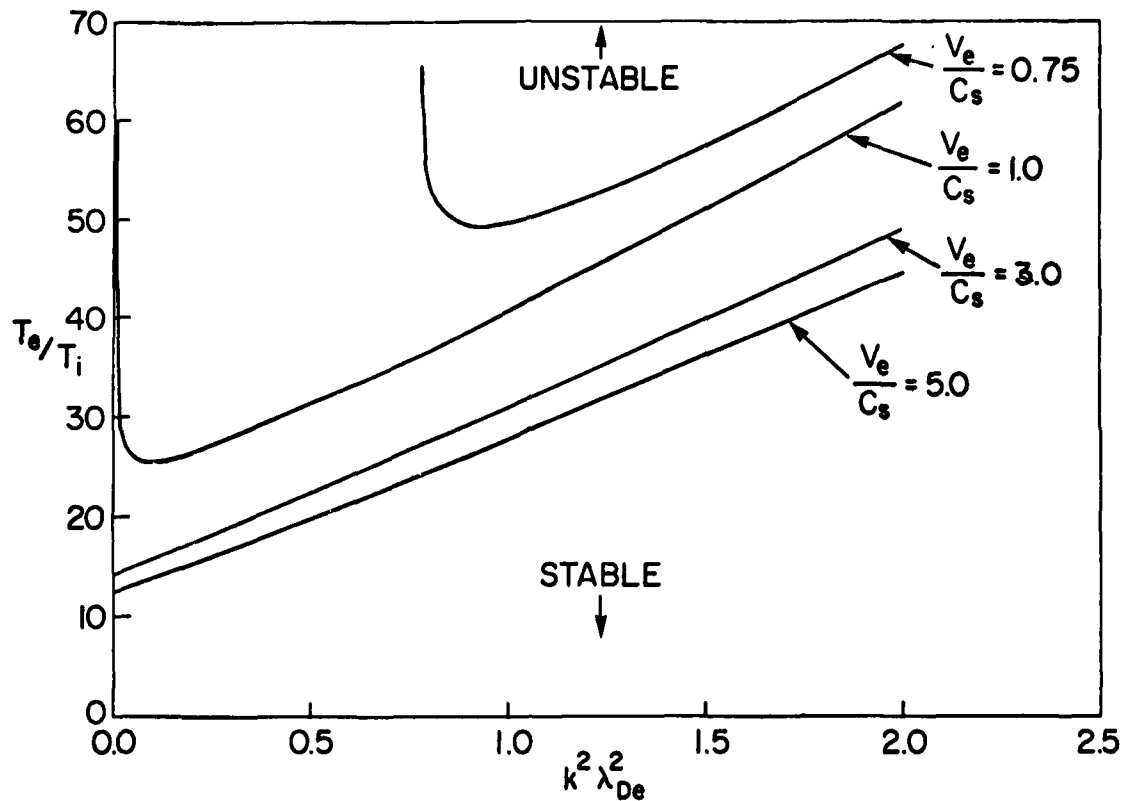


Fig. 6—Critical values of T_e/T_i for ion-acoustic instability (assuming $\nu_{ei} = 0$). Regions above the curves are unstable and below the curves are stable.

DISTRIBUTION LIST

APRIL 1981

Director
Defense Intelligence Agency
Washington, DC 20301

Attn: DTIC/D Robert I. Rubenstein 1 copy

Defense Advanced Research Project Agency
1400 Wilson Blvd.
Arlington, VA 22209
Attn: J. Bayless 1 copy

Director
Defense Nuclear Agency
Washington, DC 20305

Attn: FCPR
STVL
TISI Archives
TITL Tech. Library
J. Z. Farber (DANV)
R. L. Gullickson (RAEV) 1 copy
1 copy
1 copy
3 copies
1 copy
1 copy

Defense Technical Information Center
Cameron Station
5010 Duke Street
Alexandria, VA 22314

Attn: T. C. 12 copies

Under Sec'y of Defense for RSCH and ENRG
Department of Defense
Washington, DC 20301

Attn: SSSS(OS) 1 copy

Chief
Livermore Division Fld Command DIA
Lawrence National Laboratory
P. O. Box 808
Livermore, CA 94551

Attn: FCPL 1 copy

National Technical Information Service
U.S. Department of Commerce
5265 Port Royal Road
Springfield, VA 22161 24 copies

Commander
DMC System Command
P. O. Box 1500
Huntsville, AL 35807

Attn: SSC-TEN 1 copy

DEP Chief of Staff for RSCH DEV & ACQ
Department of the Air Force
Washington, DC 20330

Attn: DAWA-CSM-R 1 copy

Commander
Perry Diamond Laboratories
2805 Postier Mill Road
Adelphi, MD 20783
(CWNO)-1 MFR ENVELOPE: Attn: DEIHD-RBH)

Attn: DEIHD-NP
Bldg 800 J. A. Rosale 1 copy
Clynn-Bldg P. A. Caldwell 1 copy
DIXON-KBII D. Schallhorn 1 copy
DIXON-TI Tech Lib. 1 copy
S. Graybill 1 copy

Commander
Picatinny Arsenal
Dover, NJ 07801

Attn: SSPA RDI-S-E 1 copy

Commander
U. S. Army Missile Command
Redstone Arsenal, AL 35609

Attn: Redstone Scientific Information CTR
DRCFM-PM-PE-EA 1 copy

Commander
U. S. Army Nuclear Agency
7500 Eastlink Road
Building 2073
Springfield, VA 22150

Attn: ATCN-II 1 copy

Commander
U. S. Army Test and Evaluation COMD
Aberdeen Proving Ground, MD 21005

Attn: DRSTE-EL 1 copy

Commander
Naval Electronic Systems, COM HQS
Washington, DC 20360

Attn: Code 6032 1 copy

Commanding Officer
Naval Intelligence Support Center
4301 Suitland Road - Building 5
Washington, DC 20390

Attn: NISC-45 1 copy

Naval Research Laboratory
Addressed: Attn: Name/Code
Code 2103 - TIC-Distribution 25 copies
Code 4000 - J. Boris 1 copy
Code 4002 - D. Regel 1 copy
Code 4700 - T. Coffey 25 copies
Code 4707 - J. Davis 1 copy
Code 4730 - S. Podles 1 copy
Code 4740 - V. Granstein 1 copy
Code 4750 - B. Reuben 1 copy
Code 4761 - C. Kotsopoulos 1 copy
Code 4770 - Brueck-Lind 10 copies
Code 4770 - F. Young 1 copy
Code 4770 - S. Stepanchuk 1 copy
Code 4771 - D. Mueller 10 copies
Code 4773 - G. Coopersmith 10 copies
Code 4790 - D. Coleyant 1 copy
Code 4790 - I. Huber 1 copy
Code 4791 - M. Lemke 1 copy
On-Site Contractors:
Code 4770 - P. Barker (Jaycor) 1 copy
Code 4770 - S. Goldstein (Jaycor) 1 copy
Code 4770 - R. Meyer (Jaycor) 1 copy
Code 4770 - P. Oltinger (Jaycor) 1 copy
Code 4770 - F. Sandl (Jaycor) 1 copy
Code 4790 - A. Drubet (SAI) 1 copy

Officer-in-Charge
Naval Surface Weapons Center
White Oak, Silver Spring, MD 20910

Attn: Code 1073
Code WAS01 - Navy Nuc Progs Off 1 copy
1 copy

Chief of Naval Operations
Navy Department
Washington, DC 20330

Attn: R. A. Blaise 60004 1 copy

Commander
Naval Facilities Center
Chana Lake, CA 93656

Attn: Ind. 533 Tech Lib. 1 copy

AF Weapons Laboratory, AFSC
Kirtland AFB, NM 87117

Attn: CA
ELC
NT
SUL
DYP
J. Darrah
W.L. Baker

1 copy
1 copy
1 copy
1 copy
1 copy
1 copy
1 copy

HQ USAF/ED
Washington, DC 20330

Attn: RDQS**

1 copy

Director
Joint Strategic Planning Staff JCS
O/EUTI/PET
Ogden, UT 84413

Attn: JSAS

1 copy

SAMSU/DY
Post Office Box 62300
Worldwide Postal Center
Los Angeles, CA 90009
(Technological)

Attn: D-S

1 copy

SAMSU/IN
Post Office Box 62300
Worldwide Postal Center
Los Angeles, CA 90009

Attn: TMO MAJ D. S. Muskin

1 copy

SAMSU/MI
Norton AFB, CA 92403
(Minuteman)

Attn: MDRB

1 copy

SAMSU/SK
Post Office Box 92460
Worldwide Postal Center
Los Angeles, CA 90009
(Space Communications)

Attn: SKF P. H. Stadler

1 copy

U. S. Department of Energy
Division of Inertial Fusion
Washington, DC 20545

Attn: G. Canavan
J. F. Godlove
S. L. Kahalas
R. L. Schriever

1 copy
1 copy
1 copy
1 copy

Argonne National Laboratory
9700 South Cass Avenue
Argonne, Illinois 60439

Attn: G. R. Maelissen
R. J. Martin

1 copy
1 copy

Brookhaven National Laboratory
Upton, NY 11973

Attn: A. F. Kischke

1 copy

Lawrence Berkley Laboratory
Berkeley, CA 94720

Attn: D. Keefe

1 copy

Lawrence Livermore National Laboratory
P. O. Box 808
Livermore, CA 94550

Attn: L-JB
L-153
R. O. Bangerter
R. J. Briggs
E. P. Lee
J. H. Nuckolls
S. S. Yu
Tech Info Dept. L-3

1 copy
1 copy

Los Alamos National Laboratory
P. O. Box 1663
Los Alamos, NM 87545

Attn: B. B. Henderson
K. B. Perkins
L. E. Thode

1 copy
1 copy
1 copy

National Science Foundation
Mail Stop 140
Washington, DC 20550

Attn: D. Berley

1 copy

Sandia National Laboratories
P. O. Box 5000
Albuquerque, NM 87115

Attn: J. R. Freeman
S. Humphries
D. J. Johnson
G. W. Kuswa
P. S. Miller
J. P. Vandiver
G. Yonas
Doc Con for 3141 Sandia RPM Coll

1 copy
1 copy

AVCO Research and Systems Group
201 Low 11 Street
Wilmington, DE 19807

Attn: Research Lib. AR30 Rm. 7201

1 copy

BDM Corporation, Inc.
795 Jones Bridge Drive
McLean, VA 22101

Attn: Tech Lib.

1 copy

Boeing Company, The
P. O. Box 3007
Seattle, WA 98124

Attn: Aerospace Library

1 copy

Cornell University
Ithaca, NY 14850

Attn: D. A. Horner
R. R. Sudan
J. Maenchen

1 copy
1 copy
1 copy

Dikewind Industries, Inc.
1009 Bradley Drive, SE
Albuquerque, NM 87106

Attn: E. W. Davis

1 copy

EG&G, Inc.
Albuquerque Division
P. O. Box 111118
Albuquerque, NM 87114

Attn: Technical Library

1 copy

Ford Aerospace & Communications Operations Ford & Jamboree Roads Newport Beach, CA 92663 (Formerly Aeronutronic Ford Corporation)		Kaman Science Corporation P. O. Box 7463 Colorado Springs, CO 80933
Attn: Tech Info Section	1 copy	Attn: A. P. Bridges D. H. Bryce J. R. Hoffman W. E. Ware
Ford Aerospace & Communications Corp 3939 Fabian Way Palo Alto, CA 94303 (Formerly Aeronutronic Ford Corporation)		Lockheed Missiles and Space Co., Inc. 3251 Hanover Street Palo Alto, CA 94304
Attn: Library D. R. McMorrow MS G 30	1 copy 1 copy	Attn: L. F. Chase
General Electric Company Space Division Valley Forge Space Center Goddard Blvd., King of Prussia P. O. Box 8555 Philadelphia, PA 19101		Massachusetts Institute of Technology Cambridge, MA 02139
Attn: J. C. Pennington VFSC, Rm. 4230M	1 copy	Attn: R.C. Davidson G. Beloff D. Hinshelwood
General Electric Company Techno-Center for Advanced Studies 816 State Street (P. O. Drawer Q4) Santa Barbara, CA 93102		Maxwell Laboratories, Inc. 9244 Balboa Avenue San Diego, CA 92123
Attn: DASIAC	1 copy.	Attn: R. W. Clark A. C. Koch P. Korn A. R. Miller J. Pearlman
Grumman Aerospace Corporation Bethpage, NY 11714		McDonnell Douglas Corporation 5301 Bolsa Avenue Huntington Beach, CA 92647
Attn: P. Suh	1 copy	Attn: S. Schneider
Institute for Defense Analyses 401 Army-Navy Drive Arlington, VA 22202		Mission Research Corporation 1400 San Mateo Blvd. SE Albuquerque, NM 87103
Attn: IDA Librarian R. S. Smith	1 copy	Attn: D. R. Godfrey
Ion Physics Corporation South Bedford Street Curtin, MA 01503		Mission Research Corporation-San Diego P. O. Box 1203 La Jolla, CA 92038
Attn: H. Hilde	1 copy	Attn: V.A.J. Van Lint
IRI Corporation P. O. Box 81007 San Diego, CA 92138		Mission Research Corporation 735 State Street Santa Barbara, CA 93101
Attn: R. L. Mertz	1 copy	Attn: W. C. Hart C. L. Longmire
JAYCOR, Inc. 205 S. Whiting Street Alexandria, VA 22304		Northrop Corporation Electronic Division 2301 West 120th Street Hawthorne, CA 90250
Attn: J. Guillory R. Hubbard R. Sullivan D. A. Tidman	1 copy 1 copy 1 copy 1 copy	Attn: V. R. DeMartino
JAYCOR, Inc. 1401 Cerrito Del Mar Del Mar, CA 92014		Northrop Corporation Northrop Research and Technology Ctr. 3401 West Broadway Hawthorne, CA 90250
Attn: E. Wenses	1 copy	Physical Dynamics P.O. Box 556 La Jolla, CA 92037
JAYCOR, Inc. 300 Unicorn Park Drive Nashua, NH 03060		Attn: S. Jorne
Attn: H. Linnetud	1 copy	

Physics International Co. 2700 Merced Street San Leandro, CA 94577		Systems, Science and Software, Inc. P. O. Box 1620 LaJolla, CA 92038	
Attn: J. Benford B. Bernstein G. Frazier R. Genuario E. B. Goldman R. Huff A. J. Toepfer	1 copy 1 copy 1 copy 1 copy 1 copy 1 copy 1 copy	Attn: A. R. Wilson Texas Tech University P. O. Box 5404 North College Station Lubbock, TX 79417	1 copy
Pulsar Associates, Inc. 11491 Sorrento Valley Blvd. San Diego, CA 92121		Attn: T. L. Simpson TRW Defense and Space Sys Group One Space Park Redondo Beach, CA 90278	1 copy
Attn: C. H. Jones, Jr.	1 copy	Attn: Tech Info Center/S-1930 Z.G.T. Guiragossian D. Arnush	1 copy 1 copy 1 copy
Princeton Plasma Physics Laboratory James Forrestal Campus P.O. Box 451 Princeton, N.J. 08540		University of California Dept. of Physics La Jolla, CA 92093	
Attn: R. Kulsrud	1 copy	Attn: E. Brueckner W.B. Thompson	1 copy 1 copy
Pulse Sciences, Inc. 1615 Broadway, Suite 610 Oakland, CA 94612		University of California Boelter Hall 7731 Los Angeles, CA 90024	
Attn: I. Smith P. Sunic S. Putman	1 copy 1 copy 1 copy	Attn: F.F. Chen	1 copy
R&D Associates P. O. Box 9695 Marina Del Rey, CA 90291		University of California Irvine, CA 9024	
Attn: W. R. Graham, Jr. M. Grove C. MacDonald E. Martinelli	1 copy 1 copy 1 copy 1 copy	Attn: G. Benford R. Rostoker	1 copy 1 copy
R&D Associates Suite 503 1401 Wilson Blvd. Arlington, VA 22209		University of Illinois Urbana, IL 61801	
Attn: P. J. Turchi	1 copy	Attn: G. H. Miley J. T. Verdeyen	1 copy 1 copy
Science Applications, Inc. P. O. Box 2351 LaJolla, CA 92038		University of Rochester Laboratory of Laser Energy Loss River Station, Rochester 320 Rochester, NY 14627	
Attn: J. Robert Beyster	1 copy	Attn: M. J. Lubin	1 copy
Spire Corporation P. O. Box D Bedford, MA 01730		University of Scranton Dept. of Physics Scranton, PA 18510	
Attn: R. G. Little	1 copy	Attn: F. Murray	1 copy
SRI International 333 Ravenswood Avenue Menlo Park, CA 94025		U. S. Department of Energy P. O. Box 62 Oak Ridge, TN 37830	50 copies
Attn: Setsun Odairiki	1 copy	Vought Corporation Michigan Division 38111 Van Dyke Road Sterling Heights, MI 48077 (Formerly LTV Aerospace Corp.)	
Stanford University SLAC P. O. Box 4349 Stanford, CA 94099		Attn: Tech Lib	1 copy
Attn: W. B. Herrmannsfeldt	1 copy	Atomic Weapons Research Establishment Building 115 Aldermaston, Reading RG7 4FR United Kingdom	
		Attn: J. C. Martin	1 copy

Bhabha Atomic Research Centre
Bombay - 400085, India

Attn: B. K. Godwal
A. S. Paithankar

1 copy
1 copy

CEA, Centre de Etudes de Lemeil
B. P. 27
94190 Villeneuve, Saint George
France

Attn: A. Bernard
A. Jolas

1 copy
1 copy

CEA, Centre de Etudes de Valduc
P. B. 14
21120 Is-sur-Tille
France

Attn: J. Barbare
C. Bruno
N. Camarcat
C. Patou
C. Peugnet

1 copy
1 copy
1 copy
1 copy
1 copy

Centro Di Frascati
C.P.N. 65
00040 Frascati (Roma)
Italy

Attn: J.P. Rajer

Culham Laboratories
UKAEA
Eddington, Binks.
England

Attn: N. J. Peacock

1 copy

Ecole Polytechnique
Labo. PMI
91128 Palaiseau Cedex
France

Attn: J. M. Buzzi
H. Doucet

1 copy
1 copy

Ecole Polytechnique
Labo. PMI
91128 Palaiseau Cedex
France

Attn: J.M. Buzzi
H. Doucet

1 copy
1 copy

Institut d'Electronique Fondamentale
Université Paris XI-Bat. 220
F91405 Orsay
France

Attn: G. Gautherin

1 copy

Institut für Angewandte Physik
Robert Mayer Str. 2-4
D6000 Frankfurt,
West Germany

Attn: H. Dettlinghoff
H. Klein

1 copy
1 copy

Institut Fur Neutronenphysik
un Reaktortechnik
Postfach 3600
Kernforschungszentrum
D-7500 Karlsruhe 1
West Germany

Attn: H. Bluhm
H. U. Karow
W. Schmidt
K.W. Zieber

1 copy
1 copy
1 copy
1 copy

Institute of Atomic Energy
Academia Sinica
P.O. Box 2125
Beijing
People's Republic of China

Attn: W. Ganchang, Director
R. Hong

2 copies
1 copy

Institute of Laser Engineering
Osaka University
Yamadaoka
Suita
Osaka 565, Japan

Attn: K. Imasaki
S. Nakai

1 copy
1 copy

Instituto De Investigaciones Cientificas Y Tecnicas
De Las Fuerzas Armadas
Aufrielingui y Varela
V. Martelli 1003
Pcia Bs. As. - R. Argentina

Attn: N. B. Camusso

1 copy

Max-Planck-Institut für Plasmaphysik
8046 Garching bei München
West Germany

Attn: R. Trengel
J. Holman

1 copy
1 copy

Physical Research Laboratory
Navrangpura
Ahmedabad - 380009 - India

Attn: V. Ramani
P. I. John

1 copy
1 copy

Shivaji University
Kolhapur, India

Attn: L. N. Katkan

1 copy

Tokyo Institute of Technology
The Graduate School at Nagatsuta
4259 Nagatsuta, Midori-Ku
Yokohama 227, Japan

Attn: K. Ito
S. Yamaguchi

1 copy
1 copy

Weizmann Institute of Science
Rehovot, Israel

Attn: A. E. Bleaugrand
E. Kordi
Z. Zinman

1 copy
1 copy
1 copy

Bechtel Group, Inc.
P. O. Box 3165
San Francisco, CA 94119

Attn: William D. Allen

1 copy

